Temperature-dependent study of isotropic–nematic transition for a Gay–Berne fluid using density-functional theory

2007 J. Phys.: Condens. Matter 19 376101

(http://iopscience.iop.org/0953-8984/19/37/376101)

IOP PUBLISHING JOURNAL OF PHYSICS: CONDENSED MATTER

J. Phys.: Condens. Matter **19** (2007) 376101 (12pp) doi:10.1088/0953-8984/19/37/376101

Temperature-dependent study of isotropic–nematic transition for a Gay–Berne fluid using density-functional theory

Ram Chandra Singh

Department of Physics, Hindustan Institute of Technology, 32, 34 Knowledge Park-III, Greater Noida-201306, UP, India

E-mail: rcsingh_physics@yahoo.com

Received 24 March 2007, in final form 30 May 2007
Published 27 July 2007
Online at stacks.iop.org/JPhysCM/19/376101

Abstract

We have used the density-functional theory to study the effect of varying temperature on the isotropic–nematic transition of a fluid of molecules interacting via the Gay–Berne intermolecular potential. The nematic phase is found to be stable with respect to isotropic phase in the temperature range $0.80 \leqslant T^* \leqslant 1.25$. Pair correlation functions needed as input information in density-functional theory is calculated using the Percus–Yevick integral equation theory. We find that the density-functional theory is good for studying the isotropic–nematic transition in molecular fluids if the values of the pair-correlation functions in the isotropic phase are known accurately. We have also compared our results with computer simulation results wherever they are available.

1. Introduction

Liquid crystals are characterized by long-range orientational order. This order originates from the anisotropic nature of the intermolecular interactions. Detailed information about the complex interactions is not directly accessible from experiments. Such knowledge is, however, essential for the understanding of physical and chemical properties of liquid crystalline systems. Therefore, there is considerable interest in developing and improving theoretical models for inter- as well as intramolecular interactions, which can be employed in the analysis of experimental data.

A system consisting of anisotropic molecules is known to exhibit liquid crystalline phases in between the isotropic liquid and the crystalline solid. The liquid crystalline phases that commonly occur in a system of anisotropic molecules are nematic and smectic phases [1, 2]. The property of orientational ordering in the nematic liquid crystalline phase arises from the presence of anisotropic intermolecular forces. The most commonly used models for these

systems are hard ellipsoids of revolution, hard spherocylinders [3–5], a cut sphere, the Kihara core model [6, 7], and the Gay–Berne [8] model. All these are single-site models and refer to rigid molecules of cylindrical symmetry. Even for these simple models, calculating the complete phase diagram is difficult.

A realistic pair-potential between nonspherical molecules is a fairly complex theoretical object, but, just as most of our knowledge about simple fluids of spherical molecules has been deduced from the Lennard-Jones potential, much can be learned about systems of nonspherical molecules from the Gay–Berne (GB) potential [8]. The computer simulation results [9–19] show that the GB potential is capable of forming nematic, smectic A, smectic B, and an ordered solid in addition to the isotropic liquid. The variety of mesophases formed by the anisotropic molecules interacting via the GB potential has stimulated the interest of researchers. The introduction of the attractive forces into the molecular model makes the phase diagram a little more realistic; therefore, the GB potential has become a standard model for the study of liquid crystalline phases.

The intermolecular pair potential proposed by Gay and Berne can be written as

$$u(1,2) = U(\hat{\mathbf{u}}_1, \hat{\mathbf{u}}_2, \hat{\mathbf{r}}) = 4\varepsilon(\hat{\mathbf{u}}_1, \hat{\mathbf{u}}_2, \hat{\mathbf{r}})\left\{\left[\frac{\sigma_0}{r - \sigma(\hat{\mathbf{u}}_1, \hat{\mathbf{u}}_2, \hat{\mathbf{r}}) + \sigma_0}\right]^{12} - \left[\frac{\sigma_0}{r - \sigma(\hat{\mathbf{u}}_1, \hat{\mathbf{u}}_2, \hat{\mathbf{r}}) + \sigma_0}\right]^{6}\right\}. \quad (1)$$

$\hat{\mathbf{u}}_i$ is the axial vector of molecule i and $\hat{\mathbf{r}}$ is the unit vector along $\mathbf{r} = \mathbf{r}_2 - \mathbf{r}_1$, where $\mathbf{r}_1$ and $\mathbf{r}_2$ are the positions of the centers of mass of molecules 1 and 2, respectively. $\sigma(\hat{\mathbf{u}}_1, \hat{\mathbf{u}}_2, \hat{\mathbf{r}})$ and $\varepsilon(\hat{\mathbf{u}}_1, \hat{\mathbf{u}}_2, \hat{\mathbf{r}})$ are the orientation-dependent range- and strength-parameters respectively, and are defined as

$$\sigma(\hat{\mathbf{u}}_1, \hat{\mathbf{u}}_2, \hat{\mathbf{r}}) = \sigma_0\left\{1 - \frac{1}{2}\chi\left[\frac{(\hat{\mathbf{u}}_1 \cdot \hat{\mathbf{r}} + \hat{\mathbf{u}}_2 \cdot \hat{\mathbf{r}})^2}{1 + \chi(\hat{\mathbf{u}}_1 \cdot \hat{\mathbf{u}}_2)} + \frac{(\hat{\mathbf{u}}_1 \cdot \hat{\mathbf{r}} - \hat{\mathbf{u}}_2 \cdot \hat{\mathbf{r}})^2}{1 - \chi(\hat{\mathbf{u}}_1 \cdot \hat{\mathbf{u}}_2)}\right]\right\}^{-\frac{1}{2}}, \quad (2)$$

$$\varepsilon(\hat{\mathbf{u}}_1, \hat{\mathbf{u}}_2, \hat{\mathbf{r}}) = \varepsilon_0 \varepsilon^{\upsilon}(\hat{\mathbf{u}}_1, \hat{\mathbf{u}}_2)\varepsilon'^{\mu}(\hat{\mathbf{u}}_1, \hat{\mathbf{u}}_2, \hat{\mathbf{r}}), \quad (3)$$

where

$$\varepsilon(\hat{\mathbf{u}}_1, \hat{\mathbf{u}}_2) = [1 - \chi^2(\hat{\mathbf{u}}_1 \cdot \hat{\mathbf{u}}_2)^2]^{-1/2}, \quad (4)$$

and

$$\varepsilon'(\hat{\mathbf{u}}_1, \hat{\mathbf{u}}_2, \hat{\mathbf{r}}) = 1 - \frac{1}{2}\chi'\left\{\frac{(\hat{\mathbf{u}}_1 \cdot \hat{\mathbf{r}} + \hat{\mathbf{u}}_2 \cdot \hat{\mathbf{r}})^2}{1 + \chi'(\hat{\mathbf{u}}_1 \cdot \hat{\mathbf{u}}_2)} + \frac{(\hat{\mathbf{u}}_1 \cdot \hat{\mathbf{r}} - \hat{\mathbf{u}}_2 \cdot \hat{\mathbf{r}})^2}{1 - \chi'(\hat{\mathbf{u}}_1 \cdot \hat{\mathbf{u}}_2)}\right\}, \quad (5)$$

with

$$\chi = \frac{(x_0^2 - 1)}{(x_0^2 + 1)} \qquad \text{and} \qquad \chi' = \frac{(k'^{\frac{1}{\mu}} - 1)}{(k'^{\frac{1}{\mu}} + 1)},$$

where x_0 is the molecular elongation, i.e. the ratio of molecular length-to-breadth, and k' is the ratio of the potential well depths for the side-by-side and end-to-end configurations. Note that the GB potential (1) reduces to the spherical Lennard-Jones potential when both x_0 and k' are equal to unity.

The exact form of the GB potential is determined by four parameters x_0, k', μ, and υ. The original formulation, which was designed to mimic a line of four Lennard-Jones sites, had the parameters $x_0 = 3.0$, $k' = 5$, $\mu = 2$ and $\upsilon = 1$. Varying these parameters gives rise to an infinite number of Gay–Berne potentials. These have been shown to give rise to stable nematic and smectic phases. The computer simulation studies show that this potential has been widely studied for a number of parameterizations [10–19] and can be regarded as one of the most important anisotropic potentials in use at present. Some theoretical attempts have also

been made to calculate the GB phase diagram using density-functional approach, perturbation methods and virial approximations [20–24].

The purpose of this paper is to test the accuracy of the density-functional theory (DFT) by comparing some simulation results with theoretical predictions. We have used the density-functional theory of freezing to locate the isotropic–nematic transition for (reduced) temperatures $T^* \leqslant 1.25$ of the Gay–Berne liquid crystal model with the original set of parameters $\upsilon = 1$, $\mu = 2$, and anisotropy parameters $x_0 = 3.0$ and $k' = 5$. This allows us to analyze the dependence of the coexistence properties upon changes in temperature. The paper is arranged as follows. In section 2, we describe briefly the Percus–Yevick (PY) integral equation theory for the calculation of the pair-correlation functions of the isotropic phase. The essential details of the density-functional theory of freezing have been discussed in section 3. Results for the isotropic–nematic (I–N) transition for a wide range of temperatures are presented and discussed in section 4.

2. Pair-correlation functions of the isotropic phase: PY theory

The pair-correlation function (PCF) $g(1, 2)$ is related to two-particle density distribution $\rho(1, 2)$ as

$$g(1, 2) = \frac{\rho(1, 2)}{\rho(1)\rho(2)}, \tag{6}$$

where $\rho(i)$ is the single-particle density distribution. The two-particle density distribution $\rho(1, 2)$ measures the probability of finding simultaneously a molecule in a volume element $\mathrm{d}\mathbf{r}_1\,\mathrm{d}\boldsymbol{\Omega}_1$ centered at $(\mathbf{r}_1, \boldsymbol{\Omega}_1)$ and a second molecule in a volume element $\mathrm{d}\mathbf{r}_2\,\mathrm{d}\boldsymbol{\Omega}_2$ at $(\mathbf{r}_2, \boldsymbol{\Omega}_2)$. The structural information of an isotropic liquid is contained in the two-particle density distribution $\rho(1, 2)$ as the single-particle density distribution is constant, independent of position and orientation. Since for the isotropic liquid $\rho(1) = \rho(2) = \rho_f = \langle N\rangle/V$, where $\langle N\rangle$ is the average number of molecules in the volume V,

$$\rho_f^2 g(\mathbf{r}, \boldsymbol{\Omega}_1, \boldsymbol{\Omega}_2) = \rho(\mathbf{r}, \boldsymbol{\Omega}_1, \boldsymbol{\Omega}_2), \tag{7}$$

where $\mathbf{r} = \mathbf{r}_2 - \mathbf{r}_1$. In the isotropic phase, $\rho(1, 2)$ depends only on the distance $|\mathbf{r}_2 - \mathbf{r}_1| = r$, the orientation of molecules with respect to each other, and on the direction of vector $\mathbf{r}$ ($\hat{\mathbf{r}} = \mathbf{r}/r$ is a unit vector along $\mathbf{r}$).

The pair-correlation function $g(1, 2)$ of the isotropic liquid is of particular interest, as it is the lowest-order microscopic quantity that contains information about the orientational and translational structures of the system and also has direct contact with intermolecular (as well as with intramolecular) interactions. The values of $g(1, 2)$ as a function of intermolecular separation and orientations at a given temperature and density are found either by computer simulations or by solving the Ornstein–Zernike (OZ) equation

$$h(1, 2) = c(1, 2) + \rho_f \int c(1, 3)h(2, 3)\,\mathrm{d}\mathbf{3}, \tag{8}$$

where $\mathrm{d}\mathbf{3} = \mathrm{d}\mathbf{r}_3\,\mathrm{d}\boldsymbol{\Omega}_3$ and $h(1, 2) = g(1, 2) - 1$ and $c(1, 2)$ are, respectively, the total and direct pair-correlation functions (DCFs), using a suitable closure relation such as the Percus–Yevick (PY) integral equation, hypernetted chain (HNC) relations. Approximations are introduced through these closure relations [25].

The PY closure relation is written in various equivalent forms. The form adopted here is

$$c(1, 2) = f(1, 2)[g(1, 2) - c(1, 2)], \tag{9}$$

where $f(1, 2) = \exp[-\beta u(1, 2)] - 1$ is the Mayer function, $\beta = (k_\mathrm{B}T)^{-1}$ and $u(1, 2)$ is a pair potential of interaction. Since, for the isotropic liquid, DCF is an invariant pair-wise function,

it has an expansion in a body-fixed (BF) frame in terms of a basic set of rotational invariants, as

$$c(1,2) = c(r_{12}, \Omega_1, \Omega_2) = \sum_{l_1 l_2 m} c_{l_1 l_2 m}(r_{12}) Y_{l_1 m}(\Omega_1) Y_{l_2 \underline{m}}(\Omega_2), \tag{10}$$

where $\underline{m} = -m$. The coefficients $c_{l_1 l_2 m}(r_{12})$ are defined as

$$c_{l_1 l_2 m}(r_{12}) = \int c(r_{12}, \mathbf{\Omega}_1, \mathbf{\Omega}_2) Y^*_{l_1 m}(\mathbf{\Omega}_1) Y^*_{l_2 \underline{m}}(\mathbf{\Omega}_2)\, \mathrm{d}\mathbf{\Omega}_1\, \mathrm{d}\mathbf{\Omega}_2. \tag{11}$$

Expanding all the angle-dependent functions in the BF frame, the OZ equation reduces to a set of algebraic equation in Fourier space,

$$h_{l_1 l_2 m}(k) = c_{l_1 l_2 m}(k) + (-1)^m \frac{\rho_f}{4\pi} \sum_{l_3} c_{l_1 l_3 m}(k) h_{l_3 l_2 m}(k), \tag{12}$$

where the summation is over allowed values of l_3. The PY closure relation is expanded in spherical harmonics in the body-fixed or space-fixed (SF) frame. Numerically, it is easier to calculate BF harmonic coefficients than the SF harmonic coefficients. The two harmonic coefficients are related through a linear transformation,

$$A_{l_1 l_2 m}(r_{12}) = \sum_l \left[\frac{2l+1}{4\pi}\right]^{\frac{1}{2}} A_{l_1 l_2 l}(r_{12}) Cg(l_1 l_2 l; m \underline{m} 0), \tag{13}$$

or,

$$A_{l_1 l_2 l}(r_{12}) = \sum_m \left[\frac{4\pi}{2l+1}\right]^{\frac{1}{2}} A_{l_1 l_2 m}(r_{12}) Cg(l_1 l_2 l; m \underline{m} 0). \tag{14}$$

The general function $A(1,2)$ may be either $h(1,2)$ or $c(1,2)$.

The iterative numerical solution of the PCFs can be carried out in a manner described elsewhere [26, 27]. Note that in any numerical calculation we can handle only a finite number of the spherical harmonic coefficients for each orientation-dependent function. The accuracy of the results depends on this number. As the anisotropy in the shape of the molecules (or in interactions) and the value of liquid density ρ_f increases, more harmonics are needed to get proper convergence. We have found that the series becomes converged if we truncate the series at the value of l indices equal to 6 for molecules with $x_0 \leqslant 3.0$ [26]. Though it is desirable to include higher-order harmonics, i.e. for $l > 6$, this will increase the computational time manifold. Our interest is in using the data of the harmonics of PCFs for freezing transitions where low-order harmonics are generally involved. The only effect the higher-order harmonics appear to have on these low-order harmonics is to modify the finer structure of the harmonics at small values of r whose contributions to the structural parameters (to be defined later) are negligible.

We have solved the PY equation for the GB fluid with parameters $x_0 = 3.0$, $k' = 5$, $\mu = 2$ and $\upsilon = 1$ at a wide range of reduced temperatures $T^*(= k_B T/\varepsilon_0)$ and densities $\eta[= (\pi/6)\rho_f \sigma_0^3 x_0]$. In figures 1 and 2, we compare the values of $g(r) = 1 + h_{000}(r)/4\pi$ with the computer simulation results of Miguel [9] at $T^* = 1.25$ and densities $\eta = 0.455\,53$ and $0.534\,07$, respectively. Here a full line shows the computer simulation results. From these figures we find that the results obtained from the PY theory are in good qualitative agreement with the computer simulation results. However, the quantitative agreement needs improvement. Since computer simulation results are not available for other harmonics of PCFs, we do not plot them here.

In figures 3 and 4 we also plot the SF c-harmonics $c_{220}(r)$ and $c_{440}(r)$ respectively, scaled by $(4\pi)^{\frac{3}{2}}$ for $x_0 = 3.0$ and $\eta = 0.44$ found by the PY approximation at $T^* = 1.25$, 0.95 and

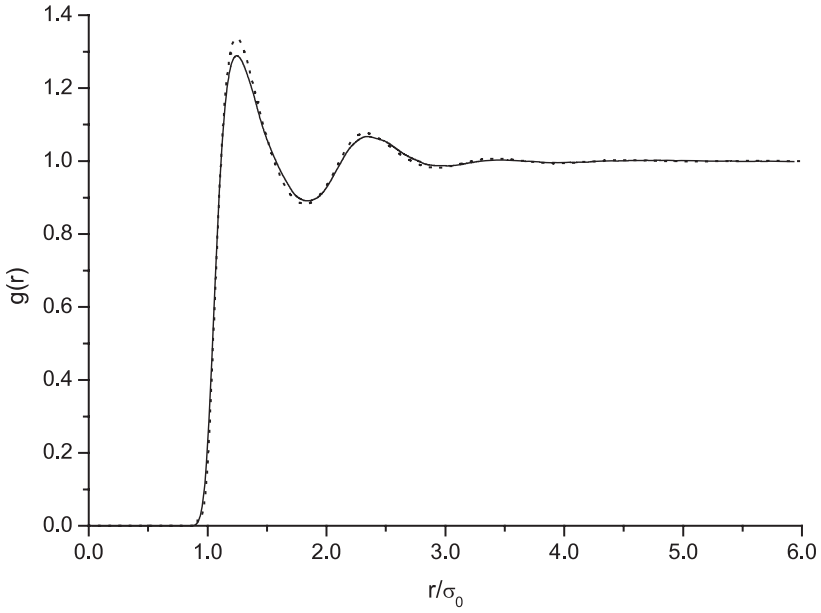

Figure 1. Pair-correlation function of the center of mass $g(r)$ for $x_0 = 3.0$, $k' = 5$, $T^* = 1.25$, and $\eta = 0.4553$. The dashed curve is our PY result and the solid curve is the simulation result of Miguel [9].

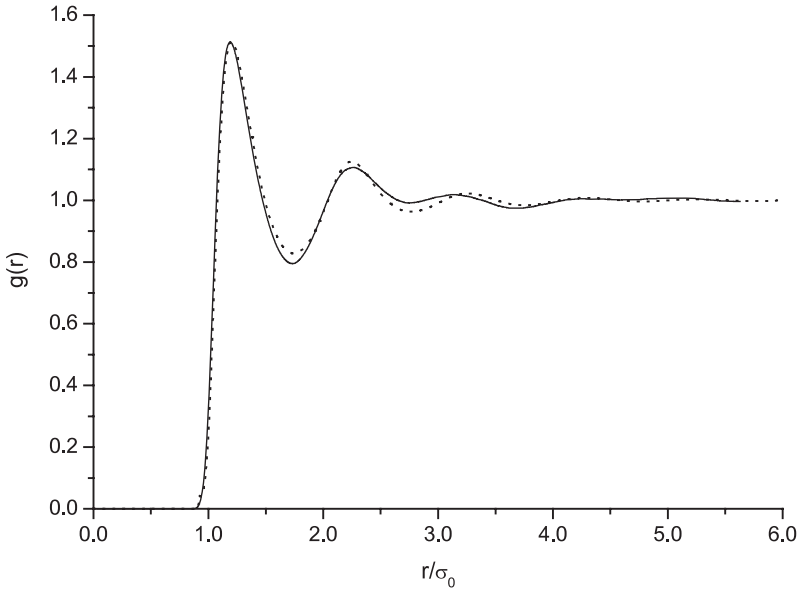

Figure 2. Same as in figure 1, but for $x_0 = 3.0$, $k' = 5$, $T^* = 1.25$, and $\eta = 0.534\,07$.

0.80. We note that these functions are short-ranged, decaying very quickly outside the region $r/\sigma_0 \geqslant 3.0$. The amplitudes of $c_{220}(r)$ and $c_{440}(r)$ within the molecular core increase slightly as T^* is lowered. These curves reveal the same nature as shown by Allen *et al* [28].

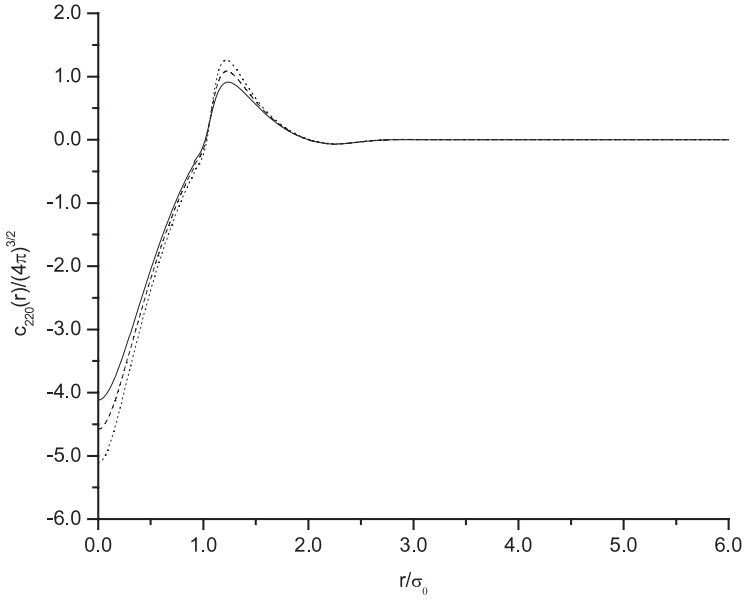

Figure 3. The SF spherical harmonic coefficient $c_{220}(r)/(4\pi)^{3/2}$ for the GB fluid at $x_0 = 3.0$, $k' = 5$, $\mu = 2$, and $\upsilon = 1$. The solid, the dashed, and the dotted curves are the PY results for $\eta = 0.44$ at $T^* = 1.25$, 0.95, and 0.80, respectively.

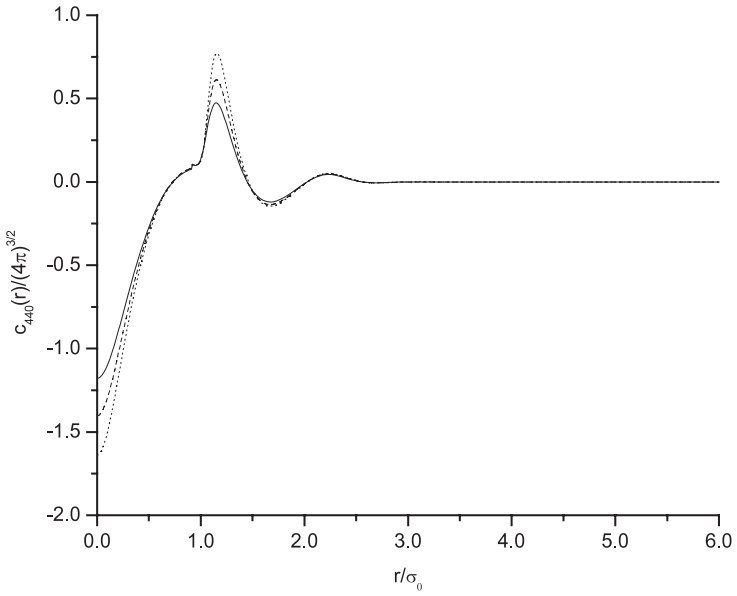

Figure 4. Same as in figure 3, but for $c_{440}(r)/(4\pi)^{3/2}$.

3. Density-functional theory of freezing

In the density-functional theory (DFT) approach, one uses the grand thermodynamic potential to locate the transition. The grand thermodynamic potential is defined as

$$-W = \beta A - \beta\mu \int \mathrm{d}\mathbf{x}\, \rho(\mathbf{x}), \tag{15}$$

where A is the Helmholtz free energy, μ is the chemical potential, and $\rho(\mathbf{x})$ is a singlet distribution function. It is convenient to subtract the isotropic fluid thermodynamic potential from W and write it as [29]

$$\Delta W = W - W_f = \Delta W_1 + \Delta W_2, \tag{16}$$

with

$$\frac{\Delta W_1}{N} = \frac{1}{\rho_f V} \int \mathrm{d}\mathbf{r}\, \mathrm{d}\Omega \left[\rho(\mathbf{r}, \Omega) \ln\left(\frac{\rho(\mathbf{r}, \Omega)}{\rho_f} \right) - \Delta\rho(\mathbf{r}, \Omega) \right], \tag{17}$$

and

$$\frac{\Delta W_2}{N} = -\frac{1}{2\rho_f} \int \mathrm{d}\mathbf{r}_{12}\, \mathrm{d}\Omega_1\, \mathrm{d}\Omega_2\, \Delta\rho(\mathbf{r}_1, \Omega_1) c(r_{12}, \Omega_1, \Omega_2) \Delta\rho(\mathbf{r}_2, \Omega_2). \tag{18}$$

Here $\Delta\rho(\mathbf{x}) = \rho(\mathbf{x}) - \rho_f$, where ρ_f is the density of the coexisting liquid.

The minimization of ΔW with respect to arbitrary variation in the ordered phase density, subject to a constraint that corresponds to some specific feature of the ordered phase, leads to

$$\ln \frac{\rho(\mathbf{r}_1, \Omega_1)}{\rho_f} = \lambda_\mathrm{L} + \int \mathrm{d}\mathbf{r}_2\, \mathrm{d}\Omega_2\, c(r_{12}, \Omega_1, \Omega_2; \rho_f) \Delta\rho(\mathbf{r}_2, \Omega_2), \tag{19}$$

where λ_L is Lagrange multiplier which appears in the equation because of constraint imposed on the minimization.

Equation (19) is solved by expanding the singlet distribution $\rho(\mathbf{x})$ in terms of the order parameters that characterize the ordered structures. One can use the Fourier series and Wigner rotation matrices to expand $\rho(\mathbf{r}, \Omega)$. Thus

$$\rho(\mathbf{r}, \Omega) = \rho_0 \sum_q \sum_{lmn} Q_{lmn}(G_q) \exp(\mathrm{i}\mathbf{G_q} \cdot \mathbf{r}) D^l_{mn}(\Omega), \tag{20}$$

where the expansion coefficients

$$Q_{lmn}(G_q) = \frac{2l+1}{N} \int \mathrm{d}\mathbf{r} \int \mathrm{d}\Omega\, \rho(\mathbf{r}, \Omega) \exp(-\mathrm{i}\mathbf{G_q} \cdot \mathbf{r}) D^{*l}_{mn}(\Omega), \tag{21}$$

are the order parameters which measure the nature and strength of the ordering, $\mathbf{G_q}$ is the reciprocal lattice vectors, ρ_0 is the mean number density of the ordered phase, and $D^{*l}_{mn}(\Omega)$ is the generalized spherical harmonics or Wigner rotation matrices [30]. Note that, for a uniaxial system consisting of cylindrically symmetric molecules, $m = n = 0$ and, therefore, one has

$$\rho(\mathbf{r}, \Omega) = \rho_0 \sum_l \sum_q Q_{lq} \exp(\mathrm{i}\mathbf{G_q} \cdot \mathbf{r}) P_l(\cos\theta), \tag{22}$$

and

$$Q_{lq} = \frac{2l+1}{N} \int \mathrm{d}\mathbf{r} \int \mathrm{d}\Omega\, \rho(\mathbf{r}, \Omega) \exp(-\mathrm{i}\mathbf{G_q} \cdot \mathbf{r}) P_l(\cos\theta), \tag{23}$$

where $P_l(\cos\theta)$ is the Legendre polynomial of degree l and θ is the angle between the cylindrical axis of the molecule and the director.

In the present calculation we consider two orientational order parameters

$$\bar{P}_l = \frac{Q_{l0}}{2l+1} = \langle P_l(\cos\theta) \rangle, \tag{24}$$

with $l = 2$ and 4: one order parameter corresponding to the positional order along the z-axis,

$$\bar{\mu} = Q_{00}(G_z) = \left\langle \cos\left(\frac{2\pi}{d} z \right) \right\rangle, \tag{25}$$

(d being the layer spacing) and one mixed-order parameter that measures the coupling between the positional and orientational ordering, defined as,

$$\tau = \frac{1}{5} Q_{20}(G_z) = \left\langle \cos\left(\frac{2\pi}{d} z\right) P_l(\cos\theta) \right\rangle. \tag{26}$$

The angular brackets in the above equations indicate the ensemble average.

The following order parameter equations are obtained by using equations (20)–(22):

$$\bar{P}_l = \frac{1}{2d} \int_0^d \mathrm{d}z_1 \int_0^\pi \sin\theta_1 \,\mathrm{d}\theta_1 \, P_l(\cos\theta_1) \exp[\mathrm{sum}], \tag{27}$$

$$\bar{\mu} = \frac{1}{2d} \int_0^d \mathrm{d}z_1 \int_0^\pi \sin\theta_1 \,\mathrm{d}\theta_1 \, \cos\left(\frac{2\pi z_1}{d}\right) \exp[\mathrm{sum}], \tag{28}$$

$$\tau = \frac{1}{2d} \int_0^d \mathrm{d}z_1 \int_0^\pi \sin\theta_1 \,\mathrm{d}\theta_1 \, P_2(\cos\theta_1) \cos\left(\frac{2\pi z_1}{d}\right) \exp[\mathrm{sum}], \tag{29}$$

and the change in density at the transition is found from the relation

$$1 + \Delta\rho^* = \frac{1}{2d} \int_0^d \mathrm{d}z_1 \int_0^\pi \sin\theta_1 \,\mathrm{d}\theta_1 \exp[\mathrm{sum}]. \tag{30}$$

Here

$$\begin{aligned} \mathrm{sum} = {} & \Delta\rho^* \hat{c}^0_{00} + 2\bar{\mu} \cos\left(\frac{2\pi z_1}{d}\right) \hat{c}^1_{00}(\theta_1) + \bar{P}_2 \hat{c}^0_{20}(\theta_1) + \bar{P}_4 \hat{c}^0_{40}(\theta_1) \\ & + 2\tau \cos\left(\frac{2\pi z_1}{d}\right) \hat{c}^1_{20}(\theta_1), \end{aligned} \tag{31}$$

and

$$\begin{aligned} \hat{c}^q_{L0}(\theta_1) = {} & \left(\frac{2l+1}{4\pi}\right)^{\frac{1}{2}} \rho_f \sum_{l_1 l} i^l (2l_1+1)^{\frac{1}{2}} (2l+1)^{\frac{1}{2}} P_{l_1}(\cos\theta_1) Cg(l_1 L l; 000) \\ & \times \int_0^\infty c_{l_1 L l}(r_{12}) j_l(G_q r_{12}) r_{12}^2 \,\mathrm{d}r_{12}, \end{aligned} \tag{32}$$

where $Cg(l_1 L l; 000)$ are the Clebsch–Gordon coefficients and $G_q = 2\pi/d$.

In the isotropic phase all the four order parameters become zero. In the nematic phase the orientational order parameters $\bar{P}_2$ and $\bar{P}_4$ become nonzero but the other two parameters $\bar{\mu}$ and τ remain zero. This is because the nematic phase has no long-range positional order. In the smectic A phase all the four order parameters are nonzero, showing that the system has both the long-range orientational and positional order along one direction. In order to evaluate the transition parameters, such as order parameters, change in density etc, equations (24)–(30) were solved self-consistently using the values of harmonics of DCFs $c_{l_1 l_2 l}(r)$ evaluated at a given temperature and density. The calculation was performed with an inter-layer spacing $d = x_0$ for the smectic A phase. By substituting these solutions in equations (16)–(18), we find the grand thermodynamic potential difference between ordered and isotropic phases, i.e.

$$-\frac{\Delta W}{N} = -\Delta\rho^* + \frac{1}{2}\Delta\rho^*(2+\Delta\rho^*)\hat{c}^0_{00} + \frac{1}{2}(\bar{P}_2^2 \hat{c}^0_{22} + \bar{P}_4^2 \hat{c}^0_{44}) + \bar{\mu}^2 \hat{c}^1_{00} + 2\bar{\mu}\tau \hat{c}^1_{20} + \tau^2 \hat{c}^1_{22}, \tag{33}$$

where

$$\begin{aligned} \hat{c}^q_{LL'} = {} & (2L+1)^{\frac{1}{2}} (2L'+1)^{\frac{1}{2}} \rho_f \sum_l i^l \left(\frac{2l+1}{4\pi}\right)^{\frac{1}{2}} Cg(LL'l; 000) \\ & \times \int_0^\infty c_{LL'l}(r_{12}) j_l(G_q r_{12}) r_{12}^2 \,\mathrm{d}r_{12}. \end{aligned} \tag{34}$$

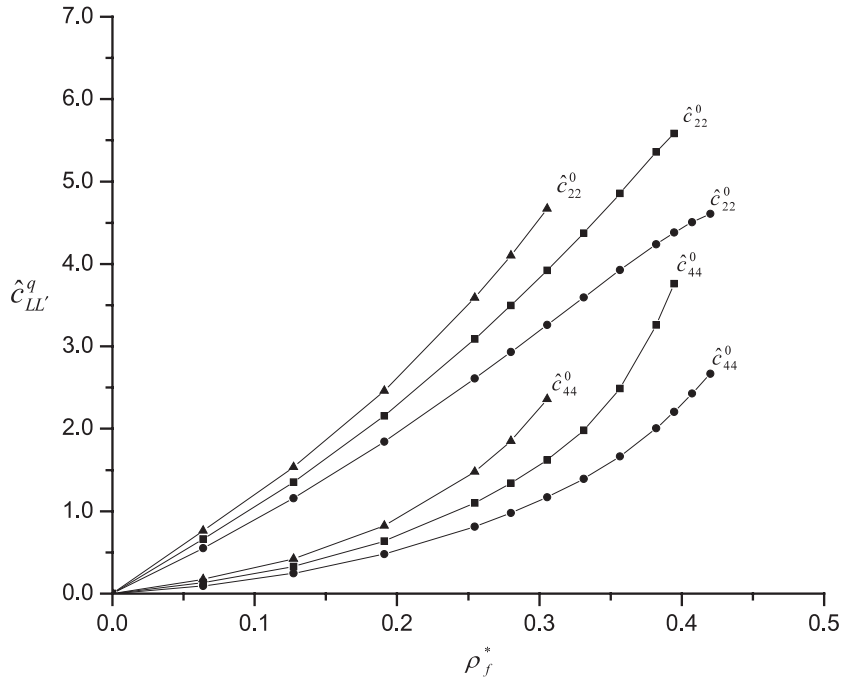

Figure 5. The structural parameter $\hat{c}^0_{LL'}$ for GB fluid at $x_0 = 3.0$, and $k' = 5$. The curves with circles, squares, and triangles are for $T^* = 1.25$, 0.95, and 0.80, respectively.

At a given temperature and density, a phase with the lowest grand potential is taken as the stable phase. Phase coexistence occurs at the values of ρ_f that makes $-\Delta W/N = 0$ for the ordered and the liquid phases.

In a theory of freezing of molecular liquids into nematic phase the structural parameters, $\hat{c}^q_{LL'}$, defined by equation (34), play an important role. The parameter $\hat{c}^0_{00}$ is related to the isothermal compressibility and $\hat{c}^0_{22}$ and higher-order coefficients to the freezing parameters. The quantity $\hat{c}^0_{22}$ and $\hat{c}^0_{44}$ are found to be very sensitive to the approximations involved in a given integral equation theory. In figure 5 we plot the structural parameters $\hat{c}^0_{LL'}$ against $\rho^*_f (= \rho_f \sigma_0^3)$ found from the PY theory for $x_0 = 3.0$ at $T^* = 0.80$, 0.95, and 1.25. It is seen from this figure that the values of $\hat{c}^0_{LL'}$ increase with density and deviate from low-density linear behaviour and increase steeply in the vicinity of the phase transition. These steep increases can in fact be related to the growth of long-range orientational correlations. Note that, as T^* increases, the phase stability increases towards higher densities and the isotropic–nematic transitions take place at higher densities.

4. Results and discussion

We have presented a thorough investigation of the temperature dependence and of the isotropic–nematic transition of the Gay–Berne liquid crystal model. The isotropic–nematic coexistence parameters of the GB fluid have been determined using the density-functional theory of freezing. The results of the theory (pressure, order parameters, and the location of the phase transition) and of several of its extensions are compared with those from computer simulation, and their relative accuracy is assessed.

Table 1. Isotropic–nematic transition parameters for the GB fluid using the harmonics of the direct pair-correlation function from the PY theory at $x_0 = 3.0$, $k' = 5$. The reduced units are $P^* = P\sigma_0^3/\varepsilon_0$, $\mu^* = \mu/\varepsilon_0$, and $\rho^* = \rho\sigma_0^3$.

T^*	Theory	ρ_f^*	ρ_n^*	$\Delta\rho^*$	$\bar{P}_2$	$\bar{P}_4$	P^*	μ^*	$\hat{c}_{22}^0$	$\hat{c}_{44}^0$
1.25	MC	0.3152	0.3219		0.55		5.20	14.50		
	DFT	0.3786	0.3820	0.009	0.682	0.381	10.93	34.35	4.198	1.956
	MWDA	0.375	0.378	0.007	0.470	0.210	10.42	32.99		
1.20	MC	0.3147	0.3213		0.52		4.92	14.32		
	DFT	0.3703	0.3740	0.001	0.680	0.377	9.31	29.65	4.206	1.924
1.15	MC	0.3129	0.3192		0.56		4.60	13.99		
	DFT	0.3617	0.3658	0.011	0.679	0.374	7.84	25.31	4.211	1.896
1.10	MC	0.3097	0.3158		0.55		4.19	13.39		
	DFT	0.3527	0.3571	0.013	0.679	0.373	6.52	21.31	4.215	1.873
1.05	MC	0.3082	0.3144		0.57		3.91	13.13		
	DFT	0.3431	0.3481	0.014	0.680	0.373	5.35	17.65	4.216	1.856
1.00	MC	0.3076	0.3128		0.52		3.63	12.79		
	DFT	0.3329	0.3386	0.017	0.684	0.376	4.31	14.31	4.213	1.844
0.95	MC	0.3045	0.3116		0.54		3.31	12.29		
	DFT	0.3219	0.3285	0.026	0.690	0.381	3.40	11.29	4.207	1.841
	MWDA	0.322	0.325	0.008	0.37	0.13	3.40	11.28		
0.90	MC	0.3015	0.3069		0.49		2.95	11.59		
	DFT	0.3099	0.3179	0.026	0.701	0.392	2.61	8.59	4.195	1.846
0.85	MC	0.3013	0.3079		0.53		2.71	11.24		
	DFT	0.2968	0.3067	0.033	0.717	0.408	1.94	6.20	4.175	1.860
0.80	MC	0.2987	0.3023		0.50		2.39	10.47		
	DFT	0.2821	0.2952	0.046	0.743	0.434	1.38	4.11	4.143	1.883
	MWDA	0.2770	0.2810	0.015	0.36	0.12	1.27	3.69		

In table 1 we list the values of the freezing parameters for I–N transition found using the density-functional theory and the simulation results of Miguel [18] for GB fluid. At lower temperature the theory shows a good agreement of the coexistence densities (ρ_f^*, ρ_n^*) with computer simulation resultss, but the agreement becomes poor as the temperature is increased. One of the possible reasons for this is the inaccuracy in the values of PCFs at higher temperatures. This is due to the fact that the PY theory underestimates the angular correlations, and this effect is more pronounced at higher temperatures than the lower temperatures. We find that the fluid freezes when the structural parameters $\hat{c}_{22}^0$ and $\hat{c}_{44}^0$ attain values $\sim$4.2 and $\sim$1.8, respectively (see table 1). Note that these numbers vary, though very weakly, with T^*; as T^* is increased, the value of $\hat{c}_{22}^0$ increases while the value of $\hat{c}_{44}^0$ decreases. The structure of the nematic phase near the transition can, therefore, be approximated as a calculable perturbation of the structure of the coexisting isotropic liquid. The short-range angular correlation that develops either due to hindered rotation or anisotropy in intermolecular interactions or due to both is already present in the isotropic phase. When this correlation grows to a certain finite value ($\hat{c}_{22}^0 \sim 4.2$), the isotropic phase becomes unstable and the system spontaneously transforms to a nematic phase that has long-range orientational ordering. An interesting feature can also be noted from table 1; the $\hat{c}_{22}^0$ ($\sim$4.2) remains almost constant at the transition as T^* is varied from 0.80 to 1.25. Note that, as T^* decreases, the phase stability decreases towards lower fluid densities and the isotropic–nematic transition take place at lower densities.

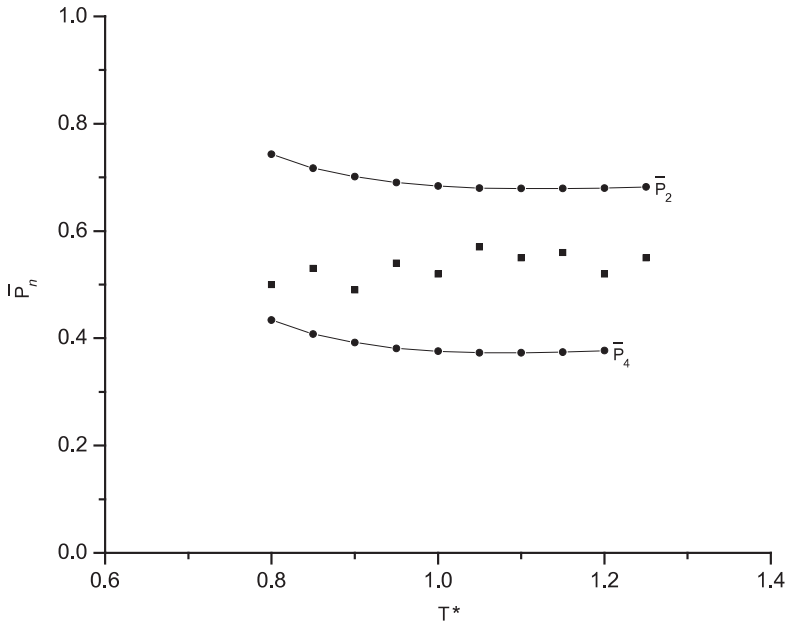

Figure 6. Variation of order parameter $\bar{P}_n$ with T^* for GB fluid at $x_0 = 3.0$, and $k' = 5$. The solid curves with circles are the results obtained from the DFT using PY values of $c(r)$. The squares are the computer simulation results of Miguel [18].

The thermodynamic stability of the nematic phase with respect to the isotropic phase has been proved for several temperatures above $T^* = 0.80$. In the range of temperatures considered here, the isotropic–nematic transition is found to be weakly first order. The densities and pressure at coexistence are found to shift to lower values as the temperature is decreased (see table 1). The theoretical results show that the coexistence densities (ρ_f^*, ρ_n^*) increase with increasing temperature, and the fractional density changes, $\Delta\rho^*$, found are rather small, which is consistent with the fact that the molecules are hard and are not very compressible at the transition densities. We observe that the values of the orientational order parameters and the change in density at the transitions are higher than those obtained by computer simulations. It has already been pointed out in our earlier work [22] that the second-order density-functional theory has the tendency to overestimate the orientational order parameters and the change in density. The density-functional theory predicts that the order parameters $\bar{P}_2$ and $\bar{P}_4$ decrease as the transition temperature is increased (figure 6). This nature reveals quite well the behaviour of the nematic order as predicted, e.g. by Maier–Saupe theory [31]. The general features of these quantities are in agreement with the experiment.

We also tried to locate the isotropic–smectic A transition using the order parameter equations (27)–(30) and energy equation (33). No evidence of smectic-like ordering has been found at any of the temperatures investigated in this work. The model includes (anisotropic) attractive interactions, and therefore allows for a systematic study of the effect of varying temperature on the liquid crystal properties.

The modified weighted-density approximation (MWDA) [32, 33] version of the density-functional method is expected to improve the agreement. We have checked it by using this theory to locate the isotropic–nematic transition at $T^* = 1.25$, 0.95, and 0.80. We find that the results of MWDA are in better agreement with computer simulation than those found from the second-order density-functional theory (see table 1).

In conclusion, we wish to emphasize that freezing transitions in complex fluids can be predicted reasonably well with the density-functional method if the values of the pair-correlation functions in the isotropic phase are known accurately. The freezing parameters are sensitive to the accuracy of harmonics of the direct-correlation functions.

Acknowledgments

We are very grateful to E de Miguel for providing the computer simulation data for comparison. The Department of Science and Technology, India supported the work through a project grant. We thank the Director and Management of Hindustan Institute of Technology, Greater Noida, for providing the necessary facilities.

References

[1] de Gennes P G and Prost J 1993 *The Physics of Liquid Crystals* (Oxford: Clarendon)
[2] Chandrasekhar S 1992 *Liquid Crystals* (Cambridge: Cambridge University Press)
[3] Frenkel D, Mulder B and McTague J P 1984 *Phys. Rev. Lett.* **52** 287
Mulder B and Frenkel D 1985 *Mol. Phys.* **55** 1193
[4] Frenkel D 1987 *J. Phys. Chem.* **91** 4912
Frenkel D 1988 *J. Phys. Chem.* **92** 3280
[5] Perera A, Kusalik P G and Patey G N 1987 *J. Chem. Phys.* **87** 1295
Perera A and Patey G N 1988 *J. Chem. Phys.* **89** 6941
[6] Kihara T 1976 *Intermolecular Forces* (New York: Wiley)
[7] Cuetos A, Martinez-Haya B and Lago S 2003 *Phys. Rev.* E **68** 011704
[8] Gay J G and Berne B J 1981 *J. Chem. Phys.* **74** 3316
[9] Chalam M K, Gubbins K E, de Miguel E and Rull L F 1991 *Mol. Simul.* **7** 357
de Miguel E, Rull L F, Chalam M K, Gubbins K E and Van Swol F 1991 *Mol. Phys.* **72** 593
de Miguel E, Rull L F, Chalam M K and Gubbins K E 1991 *Mol. Phys.* **74** 405
[10] Adams D J, Luckhurst G R and Phippen R W 1987 *Mol. Phys.* **61** 1575
Luckhurst G R, Stephens R A and Phippen R W 1990 *Liq. Cryst.* **8** 451
[11] Luckhurst G R 1993 *Ber. Bunsenges. Phys. Chem.* **97** 1
[12] Berardi R, Emerson A P J and Zannoni C 1993 *J. Chem. Soc. Faraday Trans.* **89** 4069
[13] Emsley J W, Luckhurst G R, Palke W E and Tildesley D J 1992 *Mol. Phys.* **11** 519
[14] de Miguel E, del Rio E M, Brown J T and Allen M P 1996 *J. Chem. Phys.* **105** 4234
Brown J T, Allen M P, del Rio E M and de Miguel E 1998 *Phys. Rev.* E **57** 6685
[15] Brown J T, Allen M P and Warren M 1996 *J. Phys.: Condens. Matter* **8** 9433
[16] Bates M A and Luckhurst G R 1999 *J. Chem. Phys.* **110** 7087
[17] de Miguel E and Vega C 2002 *J. Chem. Phys.* **117** 6313
[18] de Miguel E 2002 *Mol. Phys.* **100** 2449
[19] de Miguel E, del Rio E M and Bias F J 2004 *J. Chem. Phys.* **21** 11183
[20] Velasco E, Somoza A M and Mederos L 1995 *J. Chem. Phys.* **102** 8107
Velasco E and Mederos L 1998 *J. Chem. Phys.* **109** 2361
[21] Ginzburg V V, Glaser M A and Clark N A 1996 *Liq. Cryst.* **21** 265
[22] Singh R C, Ram J and Singh Y 2002 *Phys. Rev.* E **65** 031711
[23] Singh R C and Ram J 2003 *Physica* A **326** 13
[24] Singh R C 2006 *Mol. Cryst. Liq. Cryst.* **457** 67
[25] Gray C G and Gubbins K E 1984 *Theory of Molecular Fluids* (Oxford: Clarendon)
[26] Ram J, Singh R C and Singh Y 1994 *Phys. Rev.* E **49** 5117
Ram J and Singh Y 1991 *Phys. Rev.* A **44** 3718
[27] Singh R C, Ram J and Singh Y 1996 *Phys. Rev.* E **54** 977
[28] Warren M A and Allen M P 1997 *Phys. Rev. Lett.* **78** 1291
[29] Singh Y 1991 *Phys. Rep.* **207** 351 and references therein
[30] Rose M E 1957 *Elementary Theory of Angular Momemntum* (New York: Wiley)
[31] Luckhurst G R and Gray G W 1981 *The Molecular Physics of Liquid Crystals* (New York: Academic)
[32] Denton A R and Ashcroft N W 1989 *Phys. Rev.* A **39** 426
[33] Singh R C and Ram J 2006 *Physica* A **369** 493